

1998

Continuous Lake-Sediment Records of Glaciation in the Sierra Nevada between 52,600 and 12,500 14C yr B.P.

Larry Benson

University of Colorado at Boulder, great.basin666@gmail.com

Howard M. May

United States Geological Survey

Ronald C. Antweiler

United States Geological Survey

Terry I. Brinton


United States Geological Survey

Michaele Kashgarian

Lawrence Livermore National Laboratory

See next page for additional authors

Follow this and additional works at: <http://digitalcommons.unl.edu/usgsstaffpub>

 Part of the [Geology Commons](#), [Oceanography and Atmospheric Sciences and Meteorology Commons](#), [Other Earth Sciences Commons](#), and the [Other Environmental Sciences Commons](#)

Benson, Larry; May, Howard M.; Antweiler, Ronald C.; Brinton, Terry I.; Kashgarian, Michaele; Smoot, Joseph P.; and Lund, Steve P., "Continuous Lake-Sediment Records of Glaciation in the Sierra Nevada between 52,600 and 12,500 14C yr B.P." (1998). *USGS Staff - Published Research*. 795.

<http://digitalcommons.unl.edu/usgsstaffpub/795>

This Article is brought to you for free and open access by the US Geological Survey at DigitalCommons@University of Nebraska - Lincoln. It has been accepted for inclusion in USGS Staff -- Published Research by an authorized administrator of DigitalCommons@University of Nebraska - Lincoln.

Authors

Larry Benson, Howard M. May, Ronald C. Antweiler, Terry I. Brinton, Michael Kashgarian, Joseph P. Smoot, and Steve P. Lund

Continuous Lake-Sediment Records of Glaciation in the Sierra Nevada between 52,600 and 12,500 ^{14}C yr B.P.

Larry V. Benson, Howard M. May, Ronald C. Antweiler, and Terry I. Brinton

United States Geological Survey, 3215 Marine Street, Boulder, Colorado 80303-1066

Michaele Kashgarian

Lawrence Livermore National Laboratory, P.O. Box 808, Livermore, California 94550

Joseph P. Smoot

United States Geological Survey, MS 955, Reston, Virginia 22092

and

Steve P. Lund

Department of Earth Sciences, University of Southern California, Los Angeles, California 90089

Received April 1, 1998

The chemistry of the carbonate-free clay-size fraction of Owens Lake sediments supports the use of total organic carbon and magnetic susceptibility as indicators of stadial–interstadial oscillations. Owens Lake records of total organic carbon, magnetic susceptibility, and chemical composition of the carbonate-free, clay-size fraction indicate that Tioga glaciation began $\sim 24,500$ and ended by $\sim 13,600$ ^{14}C yr B.P. Many of the components of glacial rock flour (e.g., TiO_2 , MnO , BaO) found in Owens Lake sediments achieved maximum values during the Tioga glaciation when valley glaciers reached their greatest extent. Total organic carbon and SiO_2 (amorphous) concentrations reached minimum values during Tioga glaciation, resulting from decreases in productivity that accompanied the introduction of rock flour into the surface waters of Owens Lake. At least 20 stadial–interstadial oscillations occurred in the Sierra Nevada between 52,600 and 14,000 ^{14}C yr B.P. Total organic carbon data from a Pyramid Lake sediment core also indicate oscillations in glacier activity between $>39,500$ and $\sim 13,600$ ^{14}C yr B.P. Alpine glacier oscillations occurred on a frequency of ≤ 1900 yr in both basins, suggesting that millennial-scale oscillations occurred in California and Nevada during most of the past 52,600 yr. © 1998 University of Washington.

Key Words: Tioga glaciation; Sierra Nevada; Owens Lake; Pyramid Lake.

INTRODUCTION

The classical “Ice Ages” of the Pleistocene were originally defined by glaciofluvial deposits and moraines formed by expansion of northern European and North American continental

ice sheets (Kukla, 1981 and references therein). In the 1950s, Emiliani turned to the marine environment, demonstrating that $\delta^{18}\text{O}$ values of planktonic foraminifera could be used to constrain the timing, growth, and decay of the ice sheets (Emiliani, 1955). By the late 1980s, isotopic records spanning the last 1.88 myr had demonstrated the existence of 63 isotope stages equivalent to ~ 31 glaciations (Williams *et al.*, 1988).

Approaches to deciphering the history of alpine glaciation in the Sierra Nevada of California are today undergoing a similar transition from land- to water-based records. Lacustrine studies of alpine glaciation have begun to establish nearly continuous, low-resolution records for the past 400,000 yr (Menking, 1997), medium-resolution records for the past 155,000 yr (Bischoff *et al.*, 1997a), and high-resolution records for the past 52,600 ^{14}C yr B.P. (Benson *et al.*, 1996; Benson *et al.*, 1997a; Benson *et al.*, 1998).

In this paper, we compare proxy records of alpine glaciation obtained from sediment cores in the Owens and Pyramid lake basins of California and Nevada in order to define the centennial- to millennial-scale glaciation history of the Sierra Nevada for the period 52,600 to 12,500 ^{14}C yr B.P. A study of the chemistry of the carbonate-free clay-size fraction reported in this paper supports the previous use of total organic carbon and magnetic susceptibility (Benson *et al.*, 1996) as robust indicators of stade/interstade oscillations in the Owens Lake basin. Such records are critical in assessing the relation (if any) of North Atlantic temperature perturbations (Dansgaard–Oeschger cycles) to climate variability in the western United States.

THE STUDY AREA

The lake basins discussed in this paper are located between 36.2 and 40.3°N. During the Tioga glaciation, Sierran ice fields extended from 36.4 to 39.7°N (Fig. 1; Wahrhaftig and Birman, 1956) and valley glaciers formed between 36.2 and 40.2°N (Clark, 1995). The Owens Valley drainage area encompasses ~8500 km² and includes the mountain areas that extend from the crest of the Sierra Nevada to the crest of the Inyo-White mountains (Fig. 2; Hollett *et al.*, 1991). These mountains rise more than 3000 m above the valley floor, which ranges in altitude from 1067 m at Owens Lake (dry) to 1372 m at Bishop, California.

Outwash reaching Owens Lake was carried by the Owens River, which terminates at the north end of Owens Lake, and by Carroll, Cottonwood, Ash, and Braley creeks, which terminate along the western side of the lake. Pyramid Lake received outwash via the Truckee River, which drains the Lake Tahoe basin and the area north of Lake Tahoe.

Cool-season orographic precipitation, mostly from North Pacific sources, supplies most of the runoff reaching the two lake basins today. The progression of maximum precipitation along the western flank of the Sierra Nevada is associated with southward movement of the mean position of the polar jet stream (PJS) (Horn and Bryson, 1960; Pyke, 1972; Riehl *et al.*, 1954). Precipitation maxima tend to concentrate near the axis of the PJS, with precipitation decreasing rapidly south of the axis and less rapidly north of the axis (Starrett, 1949). During July and August, the westerlies weaken and Pacific storm tracks retreat north of the Sierra Nevada. During the warm season, each of the lake basins receives only a small amount of moisture in the form of convective storms originating in the Gulf of California.

During the Wisconsin Age, the PJS also played a major role in controlling the hydrologic balances of both lakes. Antevs (1938) was the first to link maximum levels of northern Great Basin lakes to the presence of a permanent ice sheet over North America, hypothesizing that the size of the Cordilleran ice sheet in western Canada, combined with a permanent high-pressure area located over it, caused storm tracks to be pushed south over central Nevada and Utah.

Renewed interest in the concept of PJS forcing of Great Basin climate occurred in the late 1980s (Benson and Thompson, 1987; Benson and Klieforth, 1989) when experiments using atmospheric general circulation models (Kutzbach and Guetter, 1986; Manabe and Broccoli, 1985) indicated that glacial-age boundary conditions, including the size and shape of the Laurentide (not Cordilleran) ice sheet, sea-surface temperatures, and land albedo were sufficient to produce the effect that Antevs had hypothesized. The PJS and the polar front form the boundary between the Northern Hemisphere Polar and Ferrel convection cells, and serve to demarcate different temperature regimes with warm air south and cold air north of the

front. The location of the PJS/polar front, therefore, played a major role in the expansion and contraction of Sierran glaciers.

PROXY INDICATORS OF ALPINE GLACIATION

Physical erosion by alpine glaciers occurs at much greater rates than by alpine streams (Hallet *et al.*, 1996), and almost all indicators of alpine glaciation directly or indirectly reflect the production of glacial rock flour and its input to a lake basin. Sediment yields from glaciated basins have generally been found to depend on extent of glacier cover; however, other glaciological variables affect sediment yields, including sliding speed, ice flux, and meltwater production (Hallet *et al.*, 1996). There are three indicators of glacier activity that will be discussed in this paper, magnetic susceptibility (MS), chemical composition of the carbonate-free clay-size fraction (CC), and total organic carbon (TOC).

Magnetic Susceptibility

Magnetic susceptibility can be used to detect the presence of glacial rock flour when the flour contains magnetic minerals such as magnetite (Fe₃O₄) (Benson *et al.*, 1996). During interglacial periods, magnetite concentrations can be diluted by autochthonous clays, carbonates, and allochthonous detrital silicates. Diagenetic processes that produce iron sulfides at the expense of primary magnetic minerals also reduce the magnetic content of lake sediments, e.g., the formation of nonmagnetic mackinawite (Fe_{1+x}S).

Diagenetic processes can also lead to the formation of secondary iron sulfides (e.g., greigite-Fe₃S₄), that have approximately the same magnetic content as the magnetite they replace. If greigite subsequently oxidizes, the MS signal associated with the greigite component is lost. The ability of MS to act as an indicator of glacier activity depends, therefore, on the location of the core site relative to the magnetic-particle delivery system and on physical and chemical processes that occur at and below the sediment-water interface.

Chemical Composition of the Carbonate-Free Clay-Size Fraction

Alpine and subalpine weathering of granitoid rocks produces grus with a grain-size distribution reflecting that of the original igneous rock; glacial abrasion of bedrock, however, produces a grain-size distribution that contains clay-size (<2μ) particles of bedrock minerals (Newton, 1991). In situations where the chemical composition of glacially derived minerals differs from the chemical composition of nonglacial allochthonous and autochthonous phases, CC will reflect glacier activity; therefore, elements unique to glacial sediments are good indicators of glacier activity (Bischoff *et al.*, 1997a).

Total Organic Carbon

Glacial rock flour dilutes the TOC fraction of lake sediment, especially near sites of surface-water discharge. Benson *et al.*

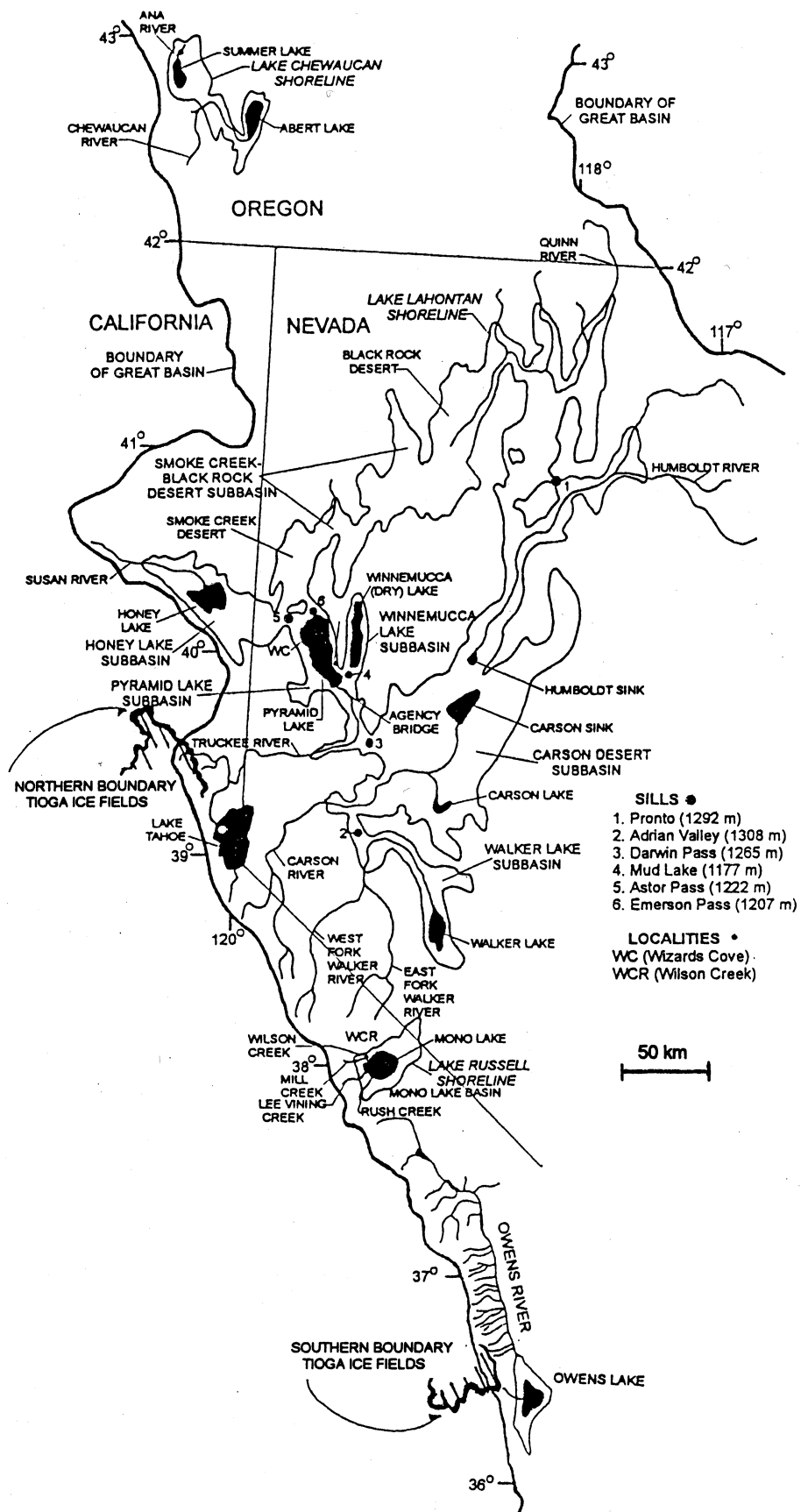


FIG. 1. Map showing location of Pyramid Lake, Mono Lake, and Owens Lake basins of California and Nevada. Latitudinal extent of Tioga glaciation (ice fields) is shown schematically (Wahrhaftig and Birman, 1956).

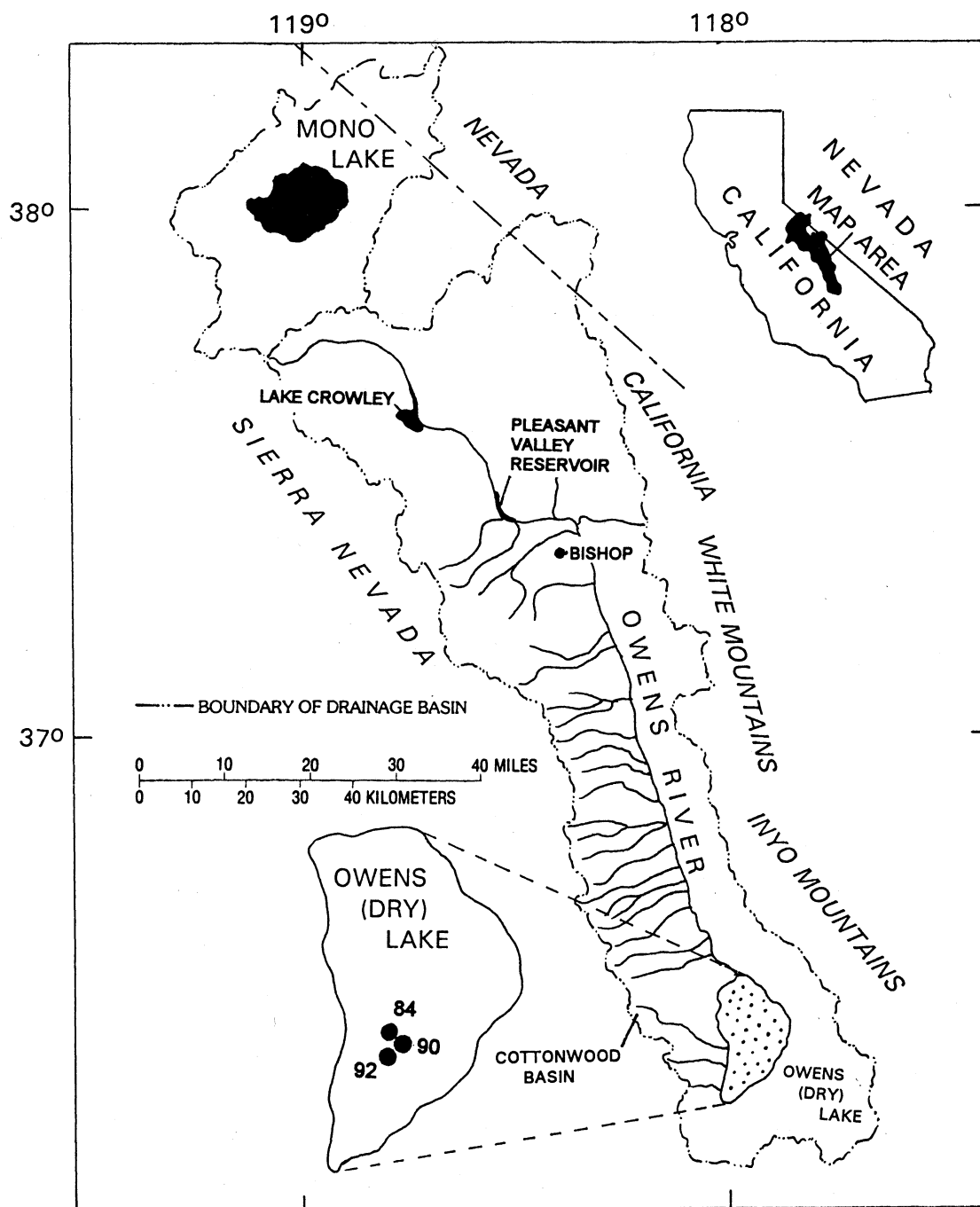
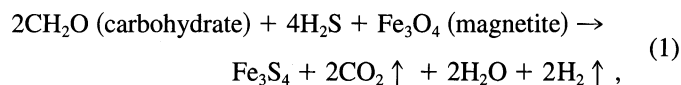


FIG. 2. Map of the Mono and Owens lake basins, showing approximate location of cores OL84, OL90-1/2, and OL92. Cores OL90-1 and -2 were taken within 200 m of each other.

(1996) have suggested that introduction of glacially derived suspended sediment also increases the turbidity of lake water, decreasing light penetration and photosynthetic production of organic carbon. Seasonal ice cover and decreased water temperature associated with cold glacial periods also decrease productivity.

Diagenetic processes can also affect the fraction of TOC in

lake sediments. Organic carbon is consumed during formation of sulfides at and below the sediment–water interface. Formation of greigite via dissolution of magnetite, i.e.,



consumes ~ 1 g of carbohydrate for every 5 g of greigite produced. In this equation, carbohydrate is used to represent the C, H, and O composition of algae and other organisms that comprise the TOC fraction of lake sediment.

Limitations of the Proxy Indicators of Alpine Glaciation

Application of the three proxies has limitations with regard to timing and extent of glaciation. Postglacial erosion and recycling of outwash and morainal and subglacial sediment can falsely signal glacier activity (e.g., Church and Ryder, 1972) for some time during and after glacier retreat (especially if the climate becomes wetter). We argue, however, that the greatest amount of rock flour is produced during the advance of Sierran glaciers and that maxima in values of the proxy indicators are temporally coincident with glacier advances.

Does the value of a proxy relate to the extent of glacier activity? We believe that the value of a proxy semiquantitatively reflects glacier extent, and in a later part of this paper we will show that the most extensive glacier advances (indicated by Tioga 2 and Tioga 3 moraines) were associated with maxima in MS and CC and minima in TOC and SiO_2 . The TOC proxy is not sensitive to the upper limit of glacier extent; i.e., TOC can potentially achieve near-zero values before rock-flour-induced turbidity reaches a maximum. If lake overflow occurs during glaciation, clay-size sediment may be carried out of the basin in the outflow, causing the intensity of glacial erosion to be underestimated. Thus, glacier advances during wet times may not be as well recorded in CC records as advances during drier times.

METHODS

Sediment cores discussed in this manuscript were collected from the south-central part of the Owens Lake basin on two occasions. In 1984, the University of Southern California (USC) obtained a 12-m core (OL84B) using a modified Livingstone-type coring device. Sediment cores OL90-1 (32.75 m) and OL90-2 (28.20 m) were obtained from the Owens Lake basin in 1990 (Fig. 2) using a truck-mounted split-spoon coring device. A continuous set of samples 5 cm in length were taken from OL90-1 and -2 spanning the time period 52,610 to 24,810 ^{14}C yr B.P. Samples 2 cm in length were taken every 3 cm from OL90-2 between levels dating 24,810 and 12,530 ^{14}C yr B.P.

Core PLC92B was taken in 7.1 m of water from the Wizards Cove area of Pyramid Lake, Nevada (Fig. 1). A continuous set of 5-cm (80-yr) samples was taken from PLC92B, excepting for a 20-cm gap below 7.9 m. The loss of the 20-cm sediment interval occurred during the penetration of the Wono tephra layer; the compact tephra layer stuck in the core barrel, displacing 20 cm of sediment that lay below it.

Soluble salts were removed from freeze-dried core (OL90-1, -2, and PLC92B) samples by repeated washing in deionized

water until the conductivity of the supernatant was $<3\times$ that of tap water. The salt-free samples were then analyzed for total inorganic carbon (TIC) and total carbon (TC) using a UIC Model 5012 CO_2 coulometer and the TOC fraction determined by difference.

Forty-eight elements were measured in the carbonate-free clay-size fraction of Owens Lake samples by inductively coupled plasma-atomic emission spectrometry (ICP-AES) and by inductively coupled plasma-mass spectrometry (ICP-MS) (Garbarino and Taylor, 1979, 1993). Separation of clay-size fractions from core samples generally followed procedures described in Jackson (1969). Two- to 12-g samples of sediment were dispersed in 125 ml of 1 M sodium acetate/acetic acid (adjusted to pH 5) at 60°C, with repeated treatments at 60° to 90°C to eliminate carbonates. Carbonate-free samples were then washed with distilled water and centrifugally size fractionated in an attempt to isolate the clay-size fraction. For Cs saturation of cation exchange sites, the sample was given three treatments with 40 ml of 0.1 M CsCl, followed by washing/centrifugation with distilled water until the supernatant appeared Cl free by test with AgNO_3 solution. Cs-saturated samples were then freeze dried and weighed. Fifty to 100 mg of the samples were microwave-digested in a sealed Teflon holding vessel, using concentrated HNO_3 , HF, and HCl in a 1:1:3 ratio. Boric acid was used to complex the excess F after digestion.

Visual inspection of clay-size residues by polarized light microscopy was performed after ICP analysis in order to pinpoint the source of SiO_2 in SiO_2 -rich samples. The inspection indicated the presence of numerous diatom fragments in those samples. The inspection also revealed that silt-size particles were present in some of the samples. The silt appears to have been incorporated in the clay-size fraction during vacuum-suctioning of the clay-bearing supernatant, and its presence may have tended to overemphasize the importance of bedrock-derived sediment (relative to smectite) in the data records generated in this study. To explore this possibility, X-ray diffraction analyses were made of eight samples that had been Mg saturated and glycolated. The X-ray patterns indicated that smectite was absent from four samples and present in minor amounts in the other four samples. These results suggest that bedrock minerals comprise almost all material present in Owens Lake sediments deposited during the last alpine glaciation.

AGE CONTROL AND RADIOCARBON RESERVOIR EFFECTS

Age control for OL90-2 is based on 26 AMS ^{14}C determinations made on the TOC fraction of cored sediment. A first-degree polynomial was fit to the youngest three ages and a second-degree polynomial was fit to all but the oldest three ages to provide age-depth models for this core (Fig. 3). The

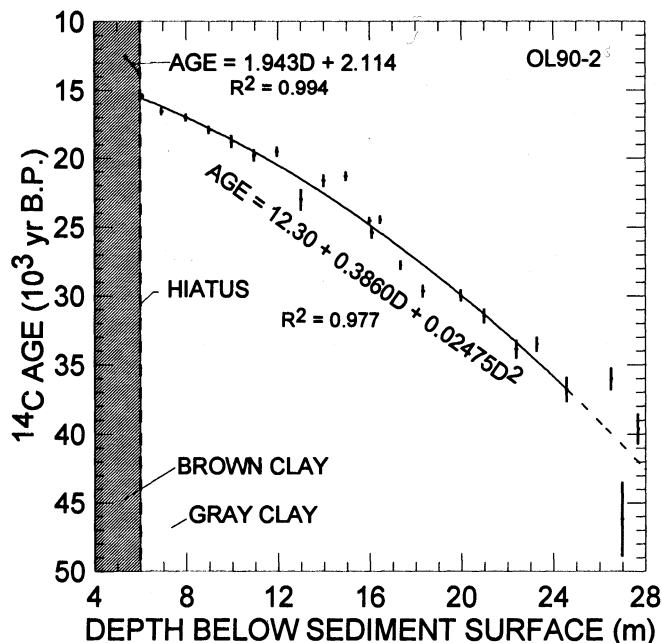


FIG. 3. Radiocarbon (^{14}C) age-depth model for OL90-2. Prior to analysis all samples were pretreated with HCL to remove inorganic carbon. The oldest three samples were not used in the polynomial fit. "D" in this and subsequent figures refers to depth. A sediment hiatus at ~ 5.94 m is indicated by an offset in the ^{14}C ages and by an abrupt change in sediment color.

hiatus at 5.94 m spans the $\leq 15,470$ to $13,660$ ^{14}C yr B.P. interval.

In order to extend age control to OL90-1, 30 MS features common to OL90-1 and -2 (Fig. 4) were matched and a second-degree polynomial was fit to the data (Fig. 5). Once equivalent OL90-2 depths for OL90-1 had been derived, the OL90-2 ^{14}C age-depth polynomial was applied to OL90-1. The age model for OL90-1 and -2 provides an unbiased interpolation between ages but treats deviations from the smoothed fit as sample noise.

An age model for the 17.35-m sediment core PLC92B was obtained by fitting a third-degree polynomial (Fig. 6) to the ^{14}C age-depth data set. Two samples (CAMS 10640 and 11989) were excluded from the fit. The relatively young ages of these samples may derive from incorporation of plant roots that penetrated the sediment during a lowstand that occurred after 26,500 ^{14}C yr B.P.

In the 1950s, Broecker and Walton (1959) found that the ^{14}C reservoir effect in Pyramid Lake was ~ 600 yr. The Pyramid Lake (Lake Lahontan) reservoir effect can also be estimated for preHolocene conditions by comparing the temporal pattern of ^{14}C plateaus observed in a recent study by Kitagawa and van der Plicht (1998) with our unpublished ^{14}C data from Pyramid Lake core PLC97-3. Kitagawa and van der Plicht (1998) documented atmospheric radiocarbon variations in varved sediments from Lake Suigetsu, Japan. An 80% decrease in $\Delta^{14}\text{C}$ occurs between 10,800 and 9800 ^{14}C yr B.P., and a 100%

decrease in $\Delta^{14}\text{C}$ occurs between 12,600 to 12,100 ^{14}C yr B.P. In core PLC97-3, these plateaus terminate at $\sim 10,200$ and $\sim 12,600$ ^{14}C yr B.P., indicating that the reservoir effect in Pyramid Lake was ~ 400 yr during the late Pleistocene (L. Benson and M. Kashgarian, unpublished data).

Extrapolation of ^{14}C dates on the TOC fraction of late-Holocene sediments from core OL84B (Fig. 7) indicate that the reservoir effect in Owens Lake was ~ 900 yr in 1913, if the sediment surface remained intact since the 1913 desiccation of the lake. Erosion has occurred in some areas; therefore, the 900-yr value may represent a maximum. Because there are no data indicating the magnitude of the reservoir effect in Owens Lake during the late Wisconsin, and because we have only a maximum estimate of the reservoir effect in the late Holocene, we elected not to alter the existing age models for cores OL90 and PLC92B.

PREVIOUS WORK

Medium-Resolution Studies of Glaciation in the Owens Lake Basin

Newton (1991) was the first to interpret the presence of quartz and feldspar in the $< 4 \mu\text{m}$ fraction in shallow cores from Owens Lake and Mono Lake as having originated from

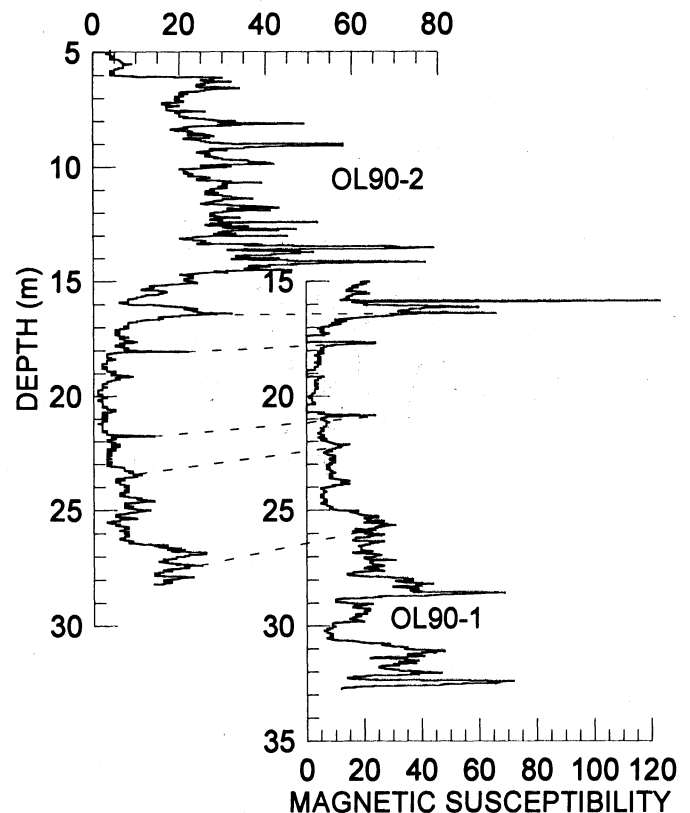


FIG. 4. Correlation of the magnetic susceptibility records between parts of OL90-1 and -2. Not all 30 correlations used in Figure 5 are shown.

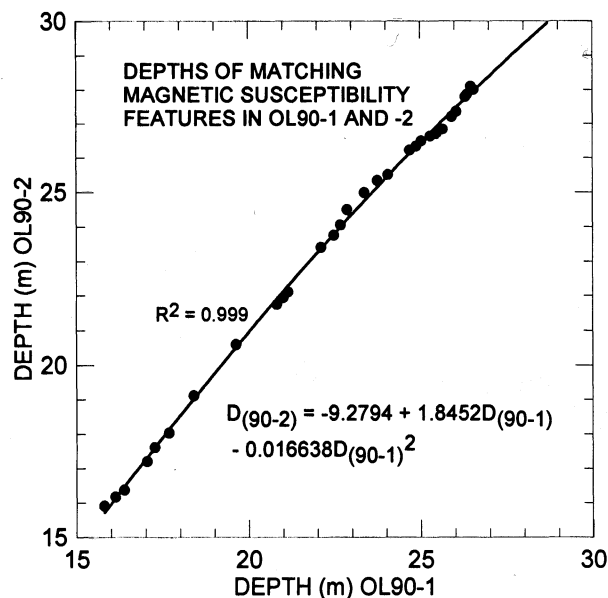


FIG. 5. Second-degree polynomial fit to MS features in OL90-1 and -2.

glacial abrasion of Sierran bedrock. Bischoff *et al.* (1997a) applied this concept in a medium-resolution study of Sierran glacial oscillations, using Na_2O , TiO_2 , BaO , and MnO components of the carbonate-free, clay-size fraction in samples from core OL92 to indicate glacial conditions. They estimated the amount of smectite, which, they argued, indicated interglacial conditions, by measuring Cs uptake in the Cs exchanged clay-size fraction.

Bischoff *et al.* (1997a) analyzed 108 samples from core OL92, each representing an interval of ~ 1500 yr (~ 60 cm). High Na_2O values indicated three glacial (g_n) intervals had occurred during the last 60,000 yr, g_3 (60,000 to 40,000 yr), g_2 (37,000 to 31,000 yr), and g_1 (27,000 to 14,000 yr).¹ Unfortunately, OL92 sediments from 6.30 to 7.27 m, 8.53 to 9.95 m, 10.75 to 12.68 m, 14.02 to 16.60 m, 17.15 to 17.75 m, and 19.10 to 20.20 m are fluidized or absent (Fig. 8). Given the degree of fluidization of the upper part of OL92, data from the upper 20 m (27,500 ^{14}C yr) will not be incorporated in this paper.

Conventional means of age control for OL92 are lacking between the top of the Bishop ash bed (759,000 yr B.P.; Sarna-Wojcicki and Pringle, 1992) at 300 m and the $30,310 \pm 310$ ^{14}C yr B.P. date (CAMS 4673-B) at 23.27 m (Fig. 8). To provide some measure of time for this interval, a constant-rate mass-accumulation model (Bischoff *et al.*, 1997b) was applied to the sediment record of OL92. In addition, ten magnetic field excursions thought to be present in core OL92 were used to validate the mass-accumulation chronology (Glen and Coe, 1997). The magnetic excursion chronology, however, has several flaws that prevent it from providing any significant con-

straint on the overall OL92 mass-accumulation chronology. Those flaws include the following: (1) only five of the ten excursions reach negative inclinations; (2) most of the negative inclinations are supported by only one or two measurements; (3) there are no declination data to help confirm the reality of the inclination-based excursions; (4) sampling was not frequent enough to characterize the normal background paleomagnetic secular variation within which each hypothesized excursion occurred; and (5) several of the excursions are coincident with fluidized zones and others overlap intervals of rotational faults caused by the coring process. These limitations make uncertain the reality of the five negative-inclination excursions and the lack of negative inclinations for the five other excursions makes it impossible to define them as such.

Detailed studies of normal paleomagnetic secular variation for the last 100,000 years (Lund, 1993; Lund *et al.*, 1988) indicate that five low (but not negative) inclinations singled out by Glen and Coe (1997) as excursions are quite common in sediment records and represent normal field variability. At least 14 possible excursions are known to have occurred during the last 780,000 yr (Keigwin *et al.*, 1997; Champion *et al.*, 1988). Even if it is assumed that the five negative inclinations are evidence of excursions, a unique assignment of the five negative inclinations to five of the 14 excursions is not possible. These arguments indicate that it is impossible to assess the accuracy of the constant-mass accumulation model developed by Bischoff *et al.* (1997b); therefore, the timing of alpine glacial events g_1 , g_2 , and g_3 may be in error by a few to several thousand years.

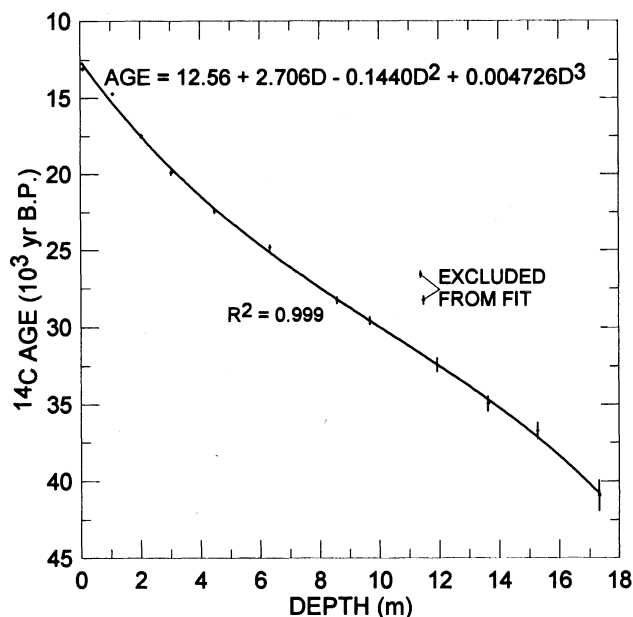


FIG. 6. Radiocarbon age-depth model for core PLC92B. Two samples excluded from the polynomial fit may have organic carbon derived from roots.

¹ The ages of these alpine glacial events are based on a constant-rate mass accumulation model; therefore, "yr" in this usage is neither ^{14}C nor calendric.

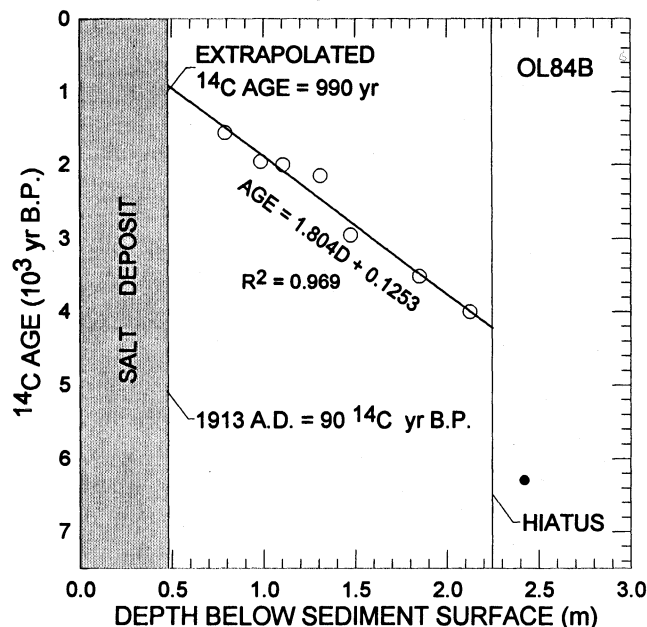


FIG. 7. Radiocarbon age-depth model for samples between 0.48 and ~2.25 m in core OL84B. The sample indicated by a filled circle was not used in the linear fit. The salt shown in the gray region was deposited ~1913 A.D. and contains mostly trona, halite, and burkeite (Dub, 1947; Smith *et al.*, 1987). The ^{14}C age at 1913 A.D. was taken from Stuiver and Becker (1993). A reservoir effect of ~900 yr was calculated from the difference between the actual and extrapolated ^{14}C ages at 1913 A.D.

High-Resolution Studies of Glaciation in the Owens Lake Basin

The MS of Owens Lake sediments derives from detrital magnetite and greigite (Fe_3S_4). Measurement of the natural remanent magnetism (NRM) of samples from the upper part of OL90-2 indicates that most samples deposited between 23,200 and 15,470 ^{14}C yr B.P. lost much of their NRM within four years after recovery (Fig. 9). Several samples from this interval were demagnetized soon after OL90-2 was recovered and their NRM measured every week for six months. A continuous loss of remanent magnetism was observed, indicating that NRM was lost during exposure of the core to the atmosphere. This progressive loss of NRM indicates that greigite was the source of most of the NRM originally present in the core. This conclusion is further supported by thermomagnetic measurements of mineral blocking temperatures (S. Lund, unpublished data). Greigite was formed in the surficial sediments of Owens Lake by alteration of other iron-bearing minerals. When core OL90 was exposed to the air, greigite oxidized and the NRM of the sediments gradually diminished.

The relatively high $\text{NRM}_1/\text{NRM}_2$ ratios of samples deposited between 13,660 and 12,500 ^{14}C yr B.P. (Fig. 9) indicate that magnetite makes up a greater part of the magnetic mineral assemblage in this interval. NRM measurements of paleomagnetic samples for the period 52,600 and 35,000 ^{14}C yr B.P. indicate a loss of only 20 to 40% of the NRM values over a

six-year period, indicating that magnetite is also the most abundant magnetic component in older sediments from OL90-1 and -2 (S. Lund, unpublished data).

High MS values characterize two intervals (52,600 to 40,000 and 25,500 to 15,470 ^{14}C yr B.P.) in core OL90 (Fig. 10a). Except for the generally low MS interval between 34,500 and 29,000 ^{14}C yr B.P., maxima in MS are associated with minima in TOC. Each of the MS maxima and TOC minima are interpreted as representing a single glacier advance (stade). During each stade, detrital silicates scoured from Sierran bedrock were washed into Owens Lake, reducing productivity and diluting the TOC fraction of Owens Lake sediments.

Both TOC and MS data sets indicate that ten stades (S-1 through S-10) occurred prior to 34,500 ^{14}C yr B.P. (Benson *et al.*, 1996). We interpret the continued oscillatory behavior of TOC between 34,500 and 29,000 ^{14}C yr to indicate the presence of minor alpine glacier advances (S-11 through S-13). The four stades that followed (S-14 through S-17), culminated in the Tioga glacial interval (24,500 to 15,470 ^{14}C yr B.P.), which is characterized by extremely high MS and extremely low TOC values (Fig. 10a). TOC values during the Tioga may also have been reduced by greigite formation (Eq. 1). We cannot completely demonstrate that the values of the proxy indicators of glacier activity (TOC and MS) quantitatively reflect glacier extent. However, the highest values of MS and lowest values of TOC occur during the glacier advances marked by the Tioga 2 and Tioga 3 moraines which mark the furthest advances of glaciers during the past 30,000 ^{14}C yr

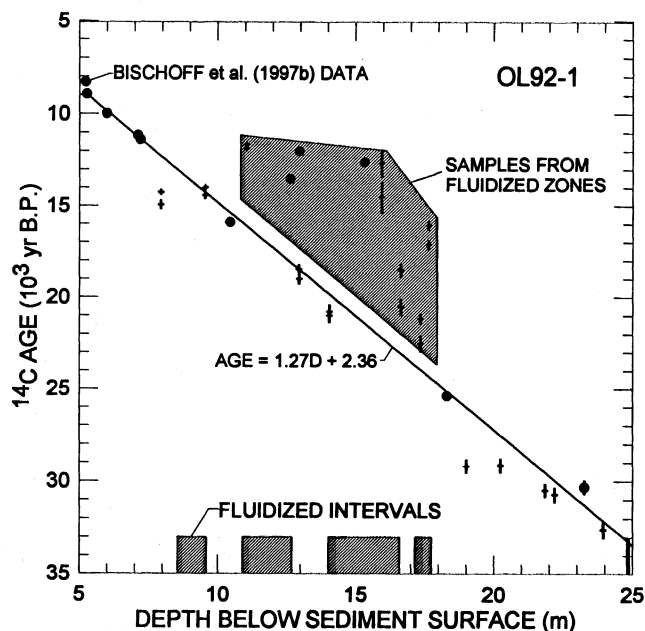


FIG. 8. Radiocarbon ages for core OL92-1. Solid circles represent data from Bischoff *et al.* (1997b); plus symbols indicate data from this report. Hatched regions indicate core intervals that are fluidized. Fluidization often entails transfer of younger sediment to lower parts of the core; therefore, ^{14}C ages of fluidized intervals are usually too young.

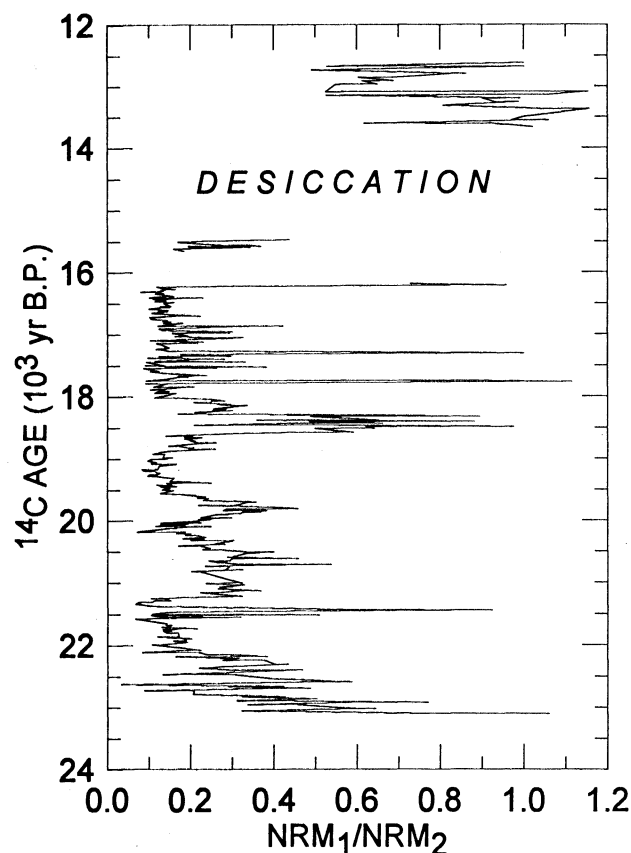


FIG. 9. Natural remanent magnetism (NRM) of samples from the upper part of OL90-2. The NRM_1/NRM_2 ratio represents replicate measurements made 4 yr apart.

(Fig. 10b; Phillips *et al.*, 1996). These observations suggest that TOC and MS values are, at least, semiquantitative indicators of glacier extent.

Comparison of Medium- and High-Resolution Records of Sierran Glaciation

In their medium-resolution study of Sierran glaciation, Bischoff *et al.* (1997a) presented evidence that Sierran glacier advance g_2 occurred between $\sim 37,000$ and $\sim 33,000$ yr B.P. They correlated the g_2 advance with the Tioga 1 moraines that the data of Phillips *et al.* (1996) suggest formed at $31,000 \pm 1000$ ^{36}Cl yr B.P. ($26,000 \pm 4500$ ^{14}C yr B.P.). The correlation of the g_2 advance with the ^{36}Cl dated Tioga 1 moraines appears unlikely because the age ranges of the two records don't overlap, even if mass accumulation ages were equivalent to ^{36}Cl ages.

Both age models (^{14}C and mass accumulation) have errors that make intercomparisons uncertain. In order to place the medium-resolution data sets within the time context of the high-resolution records, the OL90-2 ^{14}C -based chronology was transferred to OL92 using the locations of two distinctive diatom assemblages found in OL92 and OL90 (J. P. Bradbury,

personal communication, 1997).² TIC data for OL90-1 and -2 were averaged over 1000-yr intervals and plotted beside medium-resolution data records for OL92 (Fig. 11). The two medium-resolution records exhibit the same maxima in TIC at 29,000 ^{14}C yr B.P. The data sets, however, are out of phase by ~ 2000 yr at 52,000 ^{14}C yr B.P. The g_2 glacial event occurred between $\geq 38,000$ and 33,500 ^{14}C yr B.P. (Fig. 11) and is coincident with stades 8–10 (Fig. 10a), i.e., glacier advances A10–A12 depicted in Figure 3 of Benson *et al.* (1996).

APPLICATION OF THE CC APPROACH TO STADIAL-INTERSTADIAL OSCILLATIONS

One of the main objectives of this study is the comparison of the CC glacial proxy with MS and TOC glacial proxies at the stade-interstade level. To accomplish this, we analyzed the carbonate-free, clay-size fraction of 22 samples taken from many of the peaks and troughs in the TOC record of OL90-1 and -2. In general, oxide glaciation indicators (e.g., TiO_2 , MnO , BaO , and Na_2O) parallel variation in MS and mirror variation in TOC. In addition, oxide values of stades are usually elevated relative to values from adjacent interstades. Most of the oxides achieve their highest values during the Tioga glaciation (Figs. 10a, 10b). Minimum values in Na_2O and TiO_2 occur between 32,000 and 27,000 ^{14}C yr B.P. (Fig. 10a), supporting the lack of extensive glaciation during this period.

A surprising result of this analysis is that 37 of 48 elements were negatively correlated ($R^2 > 0.35$) with TOC, including all major rock-forming elements, Cs_2O , and Li_2O (Figs. 10a, 10b). In their interpretation of glacial-interglacial periods, Bischoff *et al.* (1997a) argued that values of Cs_2O and Li_2O were high during interglaciations and low during glaciations, varying inversely with Na_2O and TiO_2 on the interglacial/glacial scale. They also suggested that Cs_2O correlated with smectite abundance in the Cs exchanged clay-size fraction of Owens Lake sediment. Interglaciations were thought to mark times when Owens Lake was closed, when input of glacially derived clay-size material was absent, and when pedogenic and authigenic smectites accumulated in Owens Lake.

The compositional data for OL90-1 and -2 indicate that Cs_2O and Li_2O are poorly correlated ($R^2 = 0.08$ and 0.17) with the Na_2O glacial indicator but they are much better correlated ($R^2 = 0.48$ and 0.70) with the TiO_2 glacial indicator. Na_2O yields the poorest correlation with TOC ($R^2 = 0.35$) of all major rock-forming elements, whereas TiO_2 is negatively correlated ($R^2 = 0.78$) with TOC. These relationships suggest that Na_2O may not be as robust an indicator of glacial stages as other oxides (e.g., TiO_2) and that a process other than dilution

² *Campylodiscus clypeus* is found at 32.56 m (OL90-2 equivalent depth) in core OL90-1 and at 36.72 m in core OL92. The top of an interval of *Aulacoseira ambigua* is found at 20.21 m in core OL90-2 and 21.42 m in core OL92. These depths are equivalent to ages of 30,200 and 51,400 ^{14}C yr B.P. in core OL90-1/2.

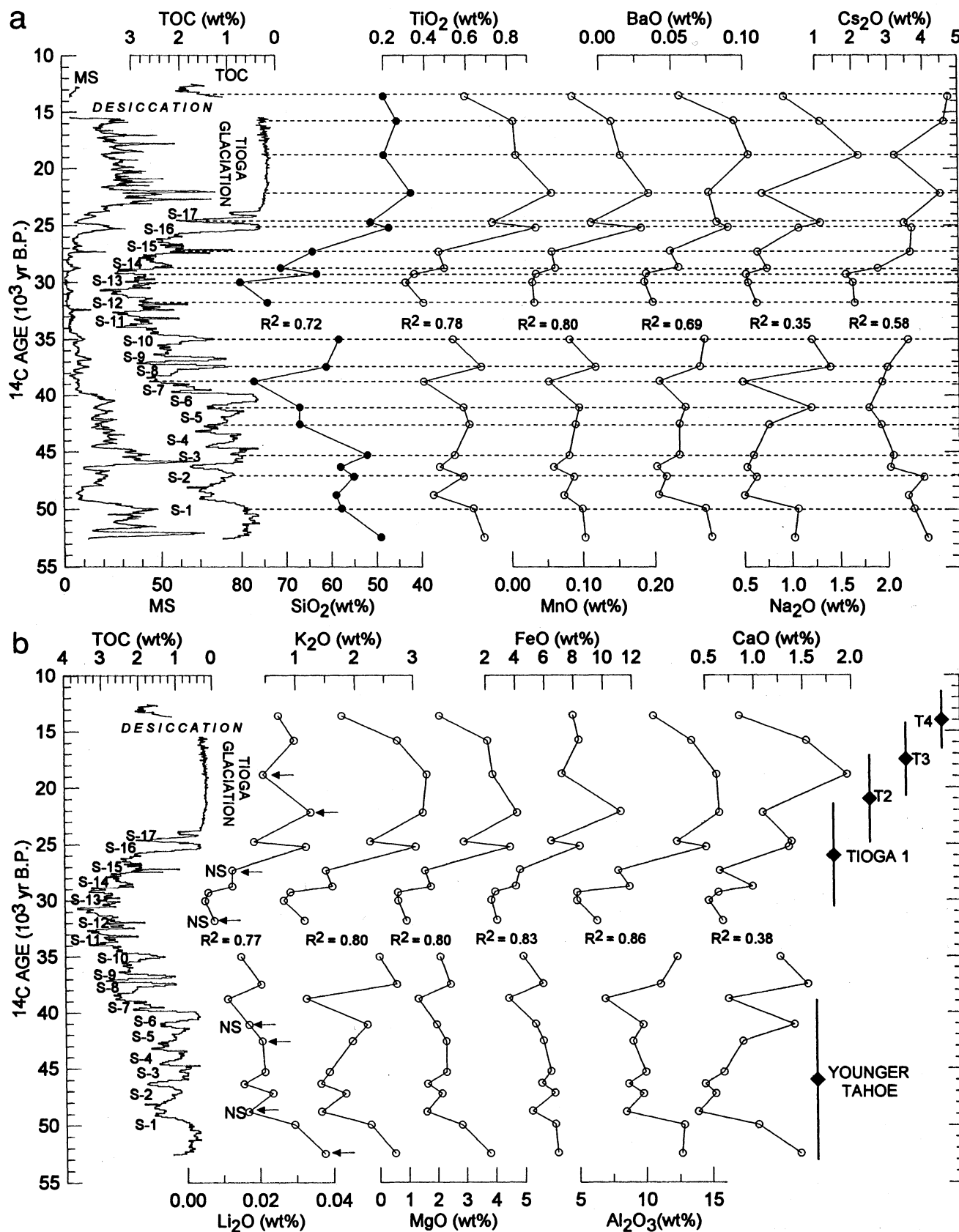


FIG. 10. (a) Magnetic susceptibility (MS), total organic carbon (TOC), and oxide analyses of OL90 sediments. Oxide analyses were made on the carbonate-free, clay-size fraction of point samples. The R^2 value indicates the correlation between the oxide component and TOC. Note that TOC and SiO₂ values increase from right to left. Horizontal dotted lines connect values of TOC used to define stades and interstades with oxide data. (b) TOC and oxide analyses of OL90 sediments compared to ^{36}Cl ages of Sierran moraines (Phillips *et al.*, 1996). The Tioga 1 data are from a moraine fragment in one small valley in the eastern Sierra and may not be meaningful in a regional sense (Douglas Clark, personal communication, 1998). The ^{36}Cl ages were converted to ^{14}C yr using the data of Bard *et al.* (1990, 1993, 1996) and Kitagawa and van der Plicht (1998). Arrows point to Mg-saturated, glycolated samples that were X-rayed. "NS" indicates the absence of expandable clay (smectite) in those samples.

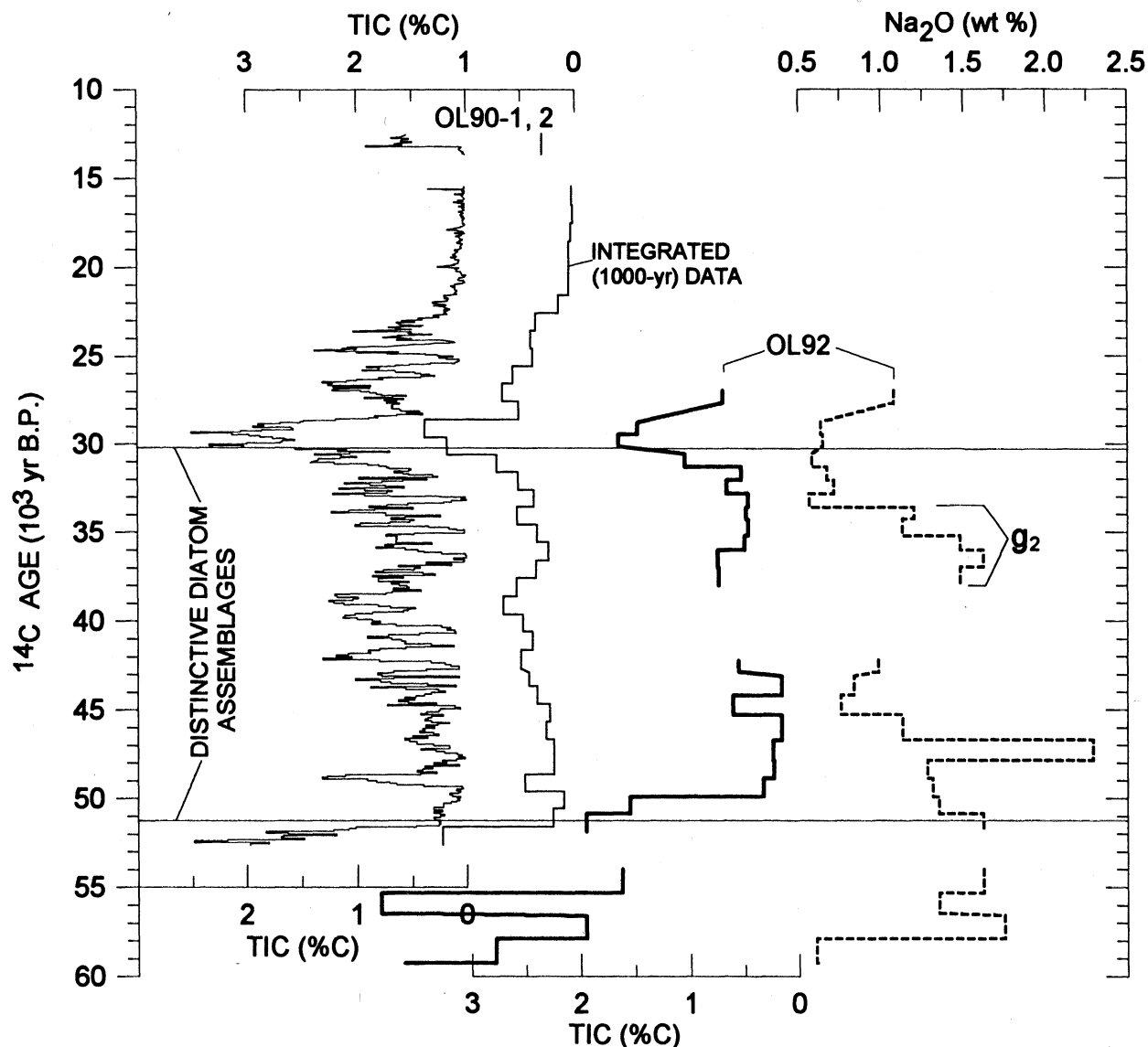


FIG. 11. High-resolution integrated (1000 yr) TIC data for OL90-1 and -2 compared with medium-resolution (~ 1500 yr) TIC (thick solid line) and Na_2O (thick dotted line) data for OL92. The OL90-2 ^{14}C based chronology was transferred to OL92 using the locations of two distinctive diatom assemblages (J. P. Bradbury, personal communication, 1998) found in OL92 and OL90-1/2. The locations of those assemblages are shown by the two solid horizontal lines. In OL90, the diatom assemblages present at depths of 20.21 and 32.56 m have ages of 30,200 and 51,140 ^{14}C yr B.P. In OL92, the diatom assemblages present at 21.42 and 36.72 m have mass-accumulation ages of 28,380 and 51,620 yr. The two medium-resolution records exhibit the same maxima in TIC at 29,000 ^{14}C yr B.P. The data sets, however, are out of phase by ~ 2000 yr at 52,000 ^{14}C yr B.P. The g_2 glacial event of Bischoff *et al.* (1997a) occurs between $\geq 38,000$ and $33,500$ ^{14}C yr B.P.

of authigenic smectites with clay-size glacial rock flour is affecting the composition of the CC between 52,600 and 15,000 ^{14}C yr B.P.

If the SiO_2 component was derived solely from bedrock silicate minerals, it would be expected to exhibit a negative correlation with some oxide components of those minerals (e.g., CaO , MgO , and $\text{FeO} + \text{Fe}_2\text{O}_3$), but it should also exhibit little or no correlation with other oxides such as Al_2O_3 , Na_2O , and K_2O (Fig. 12; Bateman, 1961). In OL90, SiO_2 varies inversely with Al_2O_3 , Na_2O , and K_2O , exhibiting a significant positive correlation with TOC ($R^2 = 0.72$). Thus, the negative

correlation of these and other elements with SiO_2 (Figs. 10a, 10b) cannot be accounted for by differences in source rock composition. We suggest that much of the SiO_2 comes from diatom fragments that are composed of amorphous SiO_2 . During stades, input of rock flour to Owens Lake would have lessened phytoplankton (diatom) productivity, decreasing the amounts of both TOC and diatom fragments (amorphous SiO_2) incorporated in lake-bottom sediments. We tested this hypothesis with X-ray diffraction analyses of two high- and two low- SiO_2 samples from OL90. The presence of a broad (amorphous SiO_2) peak centered at $\sim 22^\circ 2\theta$ in both high- SiO_2

samples (Fig. 13) demonstrates that diatom fragments were deposited during high-productivity periods and account for most of the high SiO_2 values (Figs. 10a, 10b).

The CC data, therefore, support TOC and MS as robust indicators of stage–interstage oscillations in the Owens Lake basin between 52,600 and 13,600 ^{14}C yr B.P. Interestingly, CaO and Na_2O have the poorest correlation with TOC of all major rock-forming elements ($R^2 = 0.38$ and 0.35 ; Figs. 10a and 10b) although they are highly correlated with each other ($R^2 = 0.90$). We suggest either that nonstoichiometric release of Ca and Na from plagioclase during formation of kaolinite occurred from time to time between 52,600 and 13,600 ^{14}C yr B.P. or that the ratio of plagioclase feldspar to other minerals in the clay-size fraction was not constant. In any case, CaO and Na_2O do not appear to be the best chemical proxies of glaciation during stage–interstage oscillations. An element such as Ti, which has low solubility and whose primary mineral hosts are relatively refractory, is a better and longer lived indicator of past glacier activity. During the 52,600 to 15,000 ^{14}C yr B.P. glacial interval, analyzed Cs_2O values do not appear to reflect smectite abundance; rather, they may indicate the abundance of microcline (K-feldspar), biotite, and possibly vermiculite (altered biotite), in the clay-size fraction (e.g., Hinkley, 1974).

COMPARISON OF ^{14}C AGES OF TOC-, MS-, AND CC-DEFINED STADES WITH ^{36}Cl AGES OF SIERRAN MORAINES

A ^{36}Cl study of Sierran glacial deposits by Phillips *et al.* (1996) indicated major advances at $49,000 \pm 2000$, $31,000 \pm 1000$, $25,000 \pm 1000$, $21,000 \pm 2000$, and $17,000 \pm 1000$ ^{36}Cl yr B.P. Associated systematic and random uncertainties produce a maximum combined error in such determinations of $\sim 15\%$ of the value of the measurement (Phillips *et al.*, 1997). The equivalent ^{14}C ages of these moraines ($46,000 \pm 7000$, $26,000 \pm 4500$, $21,000 \pm 3800$, $17,500 \pm 3200$, and $14,000 \pm 2500$ ^{14}C yr B.P.) obtained using the data of Bard *et al.* (1990, 1993, 1996) and Kitagawa and van der Plicht (1998) are consistent with the overall patterns in the MS and TOC data of Benson *et al.* (1996) and with the shapes of the oxide curves produced in this paper (Figs. 10a, 10b). What Phillips *et al.* (1996) termed “Younger Tahoe” moraines formed during one or more of the older stades (S-1 through S-6), and Tioga 2, 3, and 4 moraines formed during what we have termed the Tioga glaciation (Fig. 10b).

COMPARISON OF OWENS AND PYRAMID LAKE TOC RECORDS

The Pyramid Lake subbasin is one of seven subbasins that comprised Pleistocene Lake Lahontan (Fig. 1). During the Wisconsin, the level of Pyramid Lake was sometimes regulated by spill to one of three adjacent subbasins. The Mud Lake sill

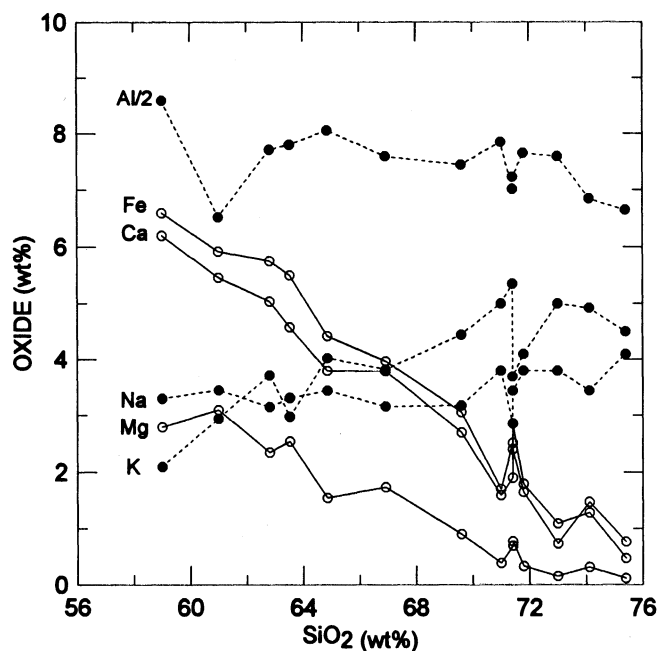


FIG. 12. Major element oxide compositions of granitoids from the east-central Sierra Nevada (Bateman, 1961). Values of Al_2O_3 were halved to fit in the figure.

(1177 m) connects Pyramid Lake to the Winnemucca Lake subbasin, the Emerson Pass sill (1207 m) connects Pyramid Lake to the Smoke Creek–Black Rock Desert subbasin, and the Darwin Pass sill (1265 m) connects Pyramid Lake to the Carson Desert subbasin.

Core PLC92B was taken in 7.1 m water from the Wizards Cove area of Pyramid Lake, Nevada (Fig. 1). A continuous set of 5-cm (80-yr) samples was taken from PLC92B, excepting a 20-cm gap below 7.9 m (loss of the 20-cm sediment interval occurred during the penetration of the Wono tephra layer; the compact tephra layer stuck in the core barrel displacing 20-cm of sediment that lay below it).

TOC data for PLC92B indicate a transition from organic-rich to organic-poor sediments at $\sim 24,500$ ^{14}C yr B.P., marking the beginning of the Tioga glaciation (Fig. 14). Prior to $\sim 24,500$ ^{14}C yr B.P., sediments from Pyramid Lake indicate millennial-scale changes in TOC. We interpret these data to indicate productivity oscillations driven by stadial–interstadial cycling. Comparison of the TOC data for the Pyramid Lake and Owens Lake basins (Fig. 14) indicates that it is difficult to correlate the oscillations from basin to basin objectively, but it is apparent that 10 to 12 oscillations occurred in each basin between 40,000 and $\sim 24,500$ ^{14}C yr B.P. It is also apparent that the start of the Tioga glaciation was recorded in both basins at nearly the same time. (See Fig. 14.)

The desiccation or lowstand of Owens Lake that occurred sometime after 15,500 ^{14}C yr B.P. (Benson *et al.*, 1996) appears to have marked the termination of the Tioga glaciation in the Owens Lake drainage. Data from OL90-1 and OL84B

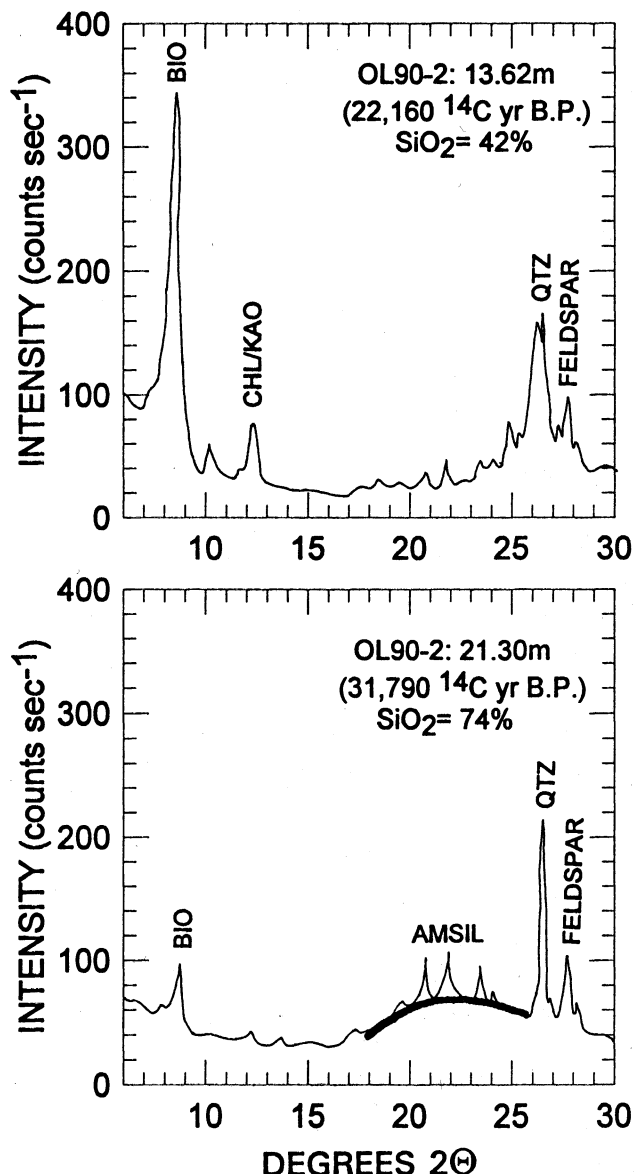


FIG. 13. X-ray diffraction patterns for a SiO_2 -poor stadial sample and a SiO_2 -rich interstadial sample from OL90. BIO refers to biotite; CHL refers to chlorite; KAO refers to kaolinite; AMSIL refers to amorphous silica; QTZ refers to quartz; and FELDSPAR refers to both microcline and plagioclase. Diatom fragments are the most probable source of amorphous SiO_2 .

(Benson *et al.*, 1996, 1997a) indicate that the desiccation terminated $13,600 \pm 100$ ^{14}C yr B.P., providing a minimum age for the end of the Tioga glaciation. TOC values for Pyramid Lake remain low after $13,600 \pm 100$ ^{14}C yr B.P. This was possibly due to continued glacier activity in the Truckee River watershed after such activity had ceased farther south, but more probably it resulted from paraglacial remobilization of glacial debris during the wet event that culminated in the Lahontan highstand ($\sim 14,000$ to $\sim 13,000$ ^{14}C yr B.P.; Benson *et al.*, 1995).

SUMMARY AND CONCLUSIONS

ICP-AES and ICP-MS analyses of the carbonate-free, clay-size fraction of 22 samples from core OL90 support the hypothesis of Benson *et al.* (1996) that millennial-scale oscillations in TOC and MS were caused by Sierran glacier (stadial-interstadial) oscillations. The work of Bischoff *et al.* (1997a) has shown that, to a first approximation, Cs_2O and Li_2O were high during alpine interglaciations and low during glaciations, varying inversely with Na_2O and TiO_2 on the interglacial/glacial scale. This study has shown that these chemical relationships do not necessarily apply to stadial/interstadial oscillations. Cs_2O and Li_2O did not reach high values during interstades; instead, their values were minima, paralleling the behavior of Na_2O and TiO_2 (and most of the other bedrock oxides). During the last alpine glaciation, most elements common to Sierran bedrock served as good indicators of stadial-interstadial oscillations because the chemistry of the carbonate-free, clay-size fraction was governed by dilution of SiO_2 (amorphous) and TOC with glacially derived silicates.

TOC data from both Owens and Pyramid lake cores indicate that Tioga glaciation began $\sim 24,500$ ^{14}C yr B.P., and TOC and

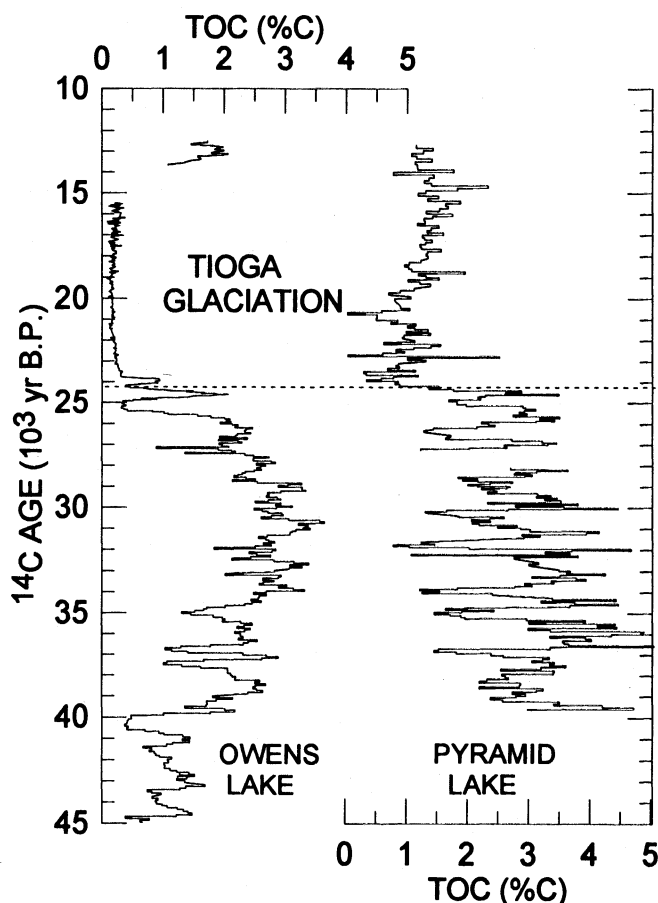


FIG. 14. TOC concentrations in samples from Owens and Pyramid lakes. Dotted line indicates the base of the Tioga glaciation.

MS data from the Owens Lake basin suggest that it ended by $\sim 13,600 \pm 100$ ^{14}C yr B.P. TOC, MS, and CC data indicate that at least 20 stadial-interstadial oscillations occurred in the Sierra Nevada between 52,600 and 14,000 ^{14}C yr B.P. These data indicate that glacier oscillations occurred on a frequency of ≤ 1900 yr.

Application of the three proxies has limitations with regard to timing and extent of glaciation. Postglacial recycling of paraglacial sediment can falsely signal glacier activity for some time during and after glacier retreat. We argue, however, that the greatest amount of rock flour is produced during the advance of Sierran glaciers and that maxima in values of the proxy indicators are coincident with glacier advances.

The value of a proxy semiquantitatively reflects glacier extent. The most extensive glacier advances in the Sierra Nevada were associated with maxima in MS and CC and minima in TOC and SiO_2 . The TOC proxy is not sensitive to the upper limit of glacier extent; i.e., TOC can potentially achieve near-zero values before rock-flour-induced turbidity reaches a maximum. If lake overflow occurs during glaciation, clay-size sediment may be carried out of the basin in the outflow, causing the intensity of glacial erosion to be underestimated. Thus, glacier advances during wet times may not be as well recorded in CC records as advances during drier times.

ACKNOWLEDGMENTS

The authors thank Jim Bischoff and Kirsten Menking for access to the medium-resolution Na and TIC data for core OL92. Helpful reviews of the manuscript were furnished by Peter Clark and Douglas Clark. J. Platt Bradbury supplied the diatom markers used to correlate OL90-1 and -2 with OL92, and Diann Miyake prepared the samples for chemical analysis.

REFERENCES

- Antevs, E. (1938). Postpluvial climatic variations in the southwest. *Bulletin of the American Meteorological Society* **19**, 190–193.
- Bard, E., Arnold, M., Fairbanks, R. G., and Hamelin, B. (1993). ^{230}Th – ^{234}U and ^{14}C ages obtained by mass spectrometry on corals. *Radiocarbon* **35**, 191–199.
- Bard, E., Hamelin, B., Arnold, M., Montaggioni, L., Cabioch, G., Faure, G., and Rougerie, F. (1996). Deglacial sea-level record from Tahiti corals and the timing of global meltwater discharge. *Nature* **382**, 241–244.
- Bard, E., Hamelin, B., Fairbanks, R. G., and Zindler, A. (1990). Calibration of the ^{14}C timescale over the past 30,000 years using mass spectrometric U–Th ages from Barbados corals. *Nature* **345**, 405–410.
- Bateman, P. C. (1961). Granitic formations in the East-Central Sierra Nevada near Bishop, California. *Geological Society of America Bulletin* **72**, 1521–1538.
- Benson, L. V., and Thompson, R. S. (1987). Lake-level variation in the Lahontan Basin for the past 50,000 years. *Quaternary Research* **28**, 69–85.
- Benson, L. V., Burdett, J., Lund, S., Kashgarian, M., and Mensing, S. (1997a). Nearly synchronous climate change in the Northern hemisphere during the last glacial termination. *Nature* **388**, 263–265.
- Benson, L. V., Burdett, J. W., Kashgarian, M., Lund, S. P., Phillips, F. M., and Rye, R. O. (1996). Climatic and hydrologic oscillations in the Owens Lake Basin and adjacent Sierra Nevada, California. *Science* **274**, 746–749.
- Benson, L. V., Kashgarian, M., and Rubin, M. (1995). Carbonate deposition, Pyramid Lake subbasin, Nevada. 2. Lake levels and polar jet stream positions reconstructed from radiocarbon ages and elevations of carbonates (tufas) deposited in the Lahontan basin. *Palaeogeography, Palaeoclimatology, Palaeoecology* **117**, 1–30.
- Benson, L. V., and Klieforth, H. (1989). Stable isotopes in precipitation and ground water in the Yucca Mountain region, southern Nevada: Paleoclimatic implications. In "Aspects of Climate Variability in the Pacific and Western Americas" (D. H. Peterson, Ed.), pp. 41–59. Geophysical Monograph 55.
- Benson, L. V., Lund, S. P., Burdett, J. W., Kashgarian, M., Rose, T. P., and Schwartz, M. (1998). Correlation of Late-Pleistocene lake-level oscillations in Mono Lake, California, with North Atlantic climate events. *Quaternary Research* **49**, 1–10.
- Benson, L. V., Smoot, J. P., Kashgarian, M., Sarna-Wojcicki, A., and Burdett, J. W. (1997b). Radiocarbon ages and environments of deposition of the Wono and Trego Hot Springs tephra layers in the Pyramid Lake subbasin, Nevada. *Quaternary Research* **47**, 251–260.
- Bischoff, J. L., Menking, K. M., Fitts, J. P., and Fitzpatrick, J. A. (1997a). Climatic oscillations 10,000–155,000 yr B.P. at Owens Lake, California, reflected in glacial rock flour abundance and lake salinity in Core OL-92. *Quaternary Research* **48**, 313–325.
- Bischoff, J. L., Stafford, T. W., and Rubin, M. (1997b). A time–depth scale for Owens Lake sediments of core OL-92: Radiocarbon dates and constant mass-accumulation rate. In "An 800,000-year paleoclimatic record from Core OL-92, Owens Lake, Southeast California" (G. I. Smith and J. L. Bischoff, Eds.), pp. 91–98. Geological Society of America Special Paper 317.
- Bond, G., Showers, W., Cheseby, M., Lotti, R., Almasi, P., deMenocal, P., Priore, P., Cullen, H., Hajdas, I., and Bonani, G. (1997). A pervasive millennial-scale cycle in North Atlantic Holocene and glacial climates. *Science* **278**, 1257–1266.
- Broecker, W. S., and Walton, A. F. (1959). The geochemistry of ^{14}C in freshwater systems. *Geochimica et Cosmochimica Acta* **16**, 15–38.
- Champion, D. E., Lanphere, M., and Kuntz, M. (1988). Evidence for a new geomagnetic reversal from lava flows in Idaho: Discussion of short polarity reversals in the Brunhes and Late Matuyama polarity chrons. *Journal of Geophysical Research* **93**, 11,667–11,680.
- Church, M., and Ryder, J. M. (1972). Paraglacial sedimentation: A consideration of fluvial processes conditioned by glaciation. *Geological Society of America Bulletin* **83**, 3059–3072.
- Clark, D. H. (1995). Extent, timing, and climatic significance of latest Pleistocene and Holocene glaciation in the Sierra Nevada, California. Unpublished doctoral thesis, University of Washington, Washington.
- Dub, G. D. (1947). Owens Lake, California—Source of sodium minerals, pp. 1–13. American Institute of Mining, Metallurgical, and Petroleum Engineers Technical Publication 2235.
- Emiliani, C. (1955). Pleistocene temperatures. *Journal of Geology* **63**, 538–578.
- Garbarino, J. R., and Taylor, H. E. (1979). An inductively coupled plasma-atomic emission spectrometric method for routine water quality testing. *Applied Spectroscopy* **33**, 220–226.
- Garbarino, J. R., and Taylor, H. E. (1993). Inductively coupled plasma-mass spectrometric method for the determination of dissolved trace elements in water. *U.S. Geological Survey Open-File Report* **94–358**.
- Glen, J. M., and Coe, R. S. (1997). Paleomagnetism and magnetic susceptibility of Pleistocene sediments from drill hole OL-92, Owens Lake, California. In "An 800,000-Year Paleoclimatic Record from Core OL-92, Owens Lake, Southeast California" (G. I. Smith and J. L. Bischoff, Eds.), pp. 67–78. Geological Society of America Special Paper 317.
- Hallet, B., Hunter, L., and Bogen, J. (1996). Rates of erosion and sediment

- evacuation by glaciers: A review of field data and their implications. *Global and Planetary Change* **12**, 213–235.
- Hinkley, T. (1974). Alkali and alkaline earth metals: Distribution and loss in a High Sierra Nevada watershed. *Geological Society of America Bulletin* **85**, 1333–1338.
- Hollett, K. J., Danskin, W. R., McCaffrey, W. F., and Walti, C. L. (1991). Geology and water resources of Owens Valley, California. In "U.S. Geological Survey Water-Supply Paper 2370."
- Horn, L. H., and Bryson, R. A. (1960). Harmonic analysis of the annual march of precipitation over the United States. *Annals of the Association of American Geographers* **50**, 157–171.
- Jackson, M. L. (1969). "Soil Chemical Analysis-Advanced Course." Dept. of Soil Science, University of Wisconsin, Madison, WI.
- Keigwin, L., Rio, D., and Acton, G. (1997). Initial reports of the ocean drilling project 172. College Station, TX.
- Kitagawa, H., and van der Plicht, J. (1998). Atmospheric radiocarbon calibration to 45,000 yr B.P.: Late glacial fluctuations and cosmogenic isotope production. *Science* **279**, 1187–1190.
- Kukla, G. J. (1981). Pleistocene Climates on Land. In "Climatic Variations and Variability: Facts and Theories" (A. Berger, Ed.), pp. 207–232. Reidel, Dordrecht.
- Kutzbach, J. E., and Guetter, P. J. (1986). The influence of changing orbital parameters and surface boundary conditions of climate simulations for the past 18,000 years. *Journal of Atmospheric Science* **43**, 1726–1759.
- Lund, S. P. (1993). Paleomagnetic secular variation. In "Trends in Geophysical Research," pp. 143–155. Council of Scientific Research Integration, Trivandrum, India.
- Lund, S. P., Liddicoat, J. C., Lajoie, K. R., Henyey, T. L., and Robinson, S. W. (1988). Paleomagnetic evidence for long-term (10^4 year) memory and periodic behavior in the earth's core dynamo process. *Geophysical Research Letters* **15**, 1101–1104.
- Manabe, S., and Broccoli, A. J. (1985). The influence of continental ice sheets on the climate of an ice age. *Journal of Geophysical Research* **90**, 2167–2190.
- Menking, K. M. (1997). Climatic signals in clay mineralogy and grain-size variations in Owens Lake core OL-92, Southeast California. An 800,000-year paleoclimatic record from Core OL-92, Owens Lake, Southeast California. *Geological Society of America Special Paper* **317**.
- Newton, M. (1991). Holocene stratigraphy and magnetostratigraphy of Owens and Mono Lakes, eastern California. Unpublished doctoral thesis, University of Southern California.
- Phillips, F. M., Zreda, M. G., Benson, L. V., Plummer, M. A., Elmore, D., and Sharma, P. (1996). Chronology for fluctuations in Late Pleistocene Sierra Nevada glaciers and lakes. *Science* **274**, 749–751.
- Phillips, F. M., Zreda, M. G., Gosse, J. C., Klein, J., Evenson, E. B., Hall, R. D., Chadwick, O. A., and Sharma, P. (1997). Cosmogenic ^{36}Cl and ^{10}Be ages of Quaternary glacial and fluvial deposits of the Wind River Range, Wyoming. *Geological Society of America Bulletin* **109**, 1453–1463.
- Pyke, C. B. (1972). Some meteorological aspects of the seasonal distribution of precipitation in the Western United States and Baja California. *University of California Water Resources Center Contribution*, **139**.
- Riehl, H., Alaka, M. A., Jordan, C. L., and Renard, R. J. (1954). The jet stream. *Meteorology and Monograph* **2**, 23–47.
- Sarna-Wojcicki, A. M., and Pringle, M. S. (1992). LaserOfusion $^{40}\text{Ar}/^{39}\text{Ar}$ ages of the tuff of Taylor Canyon and Bishop ash bed, E. California-W. Nevada. *Transactions, American Geophysical Union* **73**, 146.
- Smith, G. I., Friedman, I., and McLaughlin, R. J. (1987). Studies of quaternary saline lakes—III. Mineral, chemical, and isotopic evidence of salt solution and crystallization process in Owens Lake, California, 1969–1971. *Geochimica et Cosmochimica Acta* **51**, 811–827.
- Starrett, L. G. (1949). The relation of precipitation patterns in North America to certain types of jet streams at the 300-millibar level. *Journal of Meteorology* **6**, 347–352.
- Stuiver, M., and Becker, B. (1993). High-precision decadal calibration of the radiocarbon time scale, AD 1950–6000 BC. *Radiocarbon* **35**, 35–65.
- Wahrhaftig, C., and Birm, J. H. (1956). The Quaternary of the Pacific Mountain system in California. In "Means of Correlation of Quaternary Successions. Vol. 8, Proceedings, VII Congress International Association for Quaternary Research" (R. Morrison and H. E. Wright, Jr., Eds.), p. 293. University of Utah Press, Salt Lake City, Utah.
- Williams, D. F., Thunell, R. C., Tappa, E., Rio, D., and Raffi, I. (1988). Chronology of the Pleistocene oxygen isotope record: 0–1.88 m.y. B.P. *Palaeogeography, Palaeoclimatology, Palaeoecology* **64**, 221–240.